Eigenvalue-Based Thermoacoustic Stability and Thermal Mode Analysis of Liquid Rocket Engine Combustion Chambers and Nozzles

Sharjeel Malik | Justin Della

Faculty Advisor: Dr. Ronald Adams

Embry Riddle Aeronautical University – Daytona Beach Campus

Abstract

Combustion instability in liquid rocket engines is driven by coupling acoustic pressure oscillations and unsteady heat release. To achieve specific desired outcomes, small perturbations can be made to either decay or grow, depending on system dynamics and artificial parameters. Using a linearized eigenvalue framework, where eigenvalues determine growth/decay rates and frequencies, and eigenvectors describe spatial mode shapes and couplings between pressure, velocity, and heat release, a mathematical model can be derived to describe said behavior for a cross-section of the rocket engine. The Rayleigh criterion is a method to identify conditions under which energy is added to oscillations, while it is recommended that flame transfer functions are used for time-delay effects that lead to Helmholtz-type eigenvalue problems. Based on the Rayleigh criterion, the thermal behavior is thus modeled separately using the heat equation with internal heat generation. The solution is then decomposed into steady-state and transient components, with the transient solved via separation of variables and eigenfunction expansions. The same method and boundaries are applied to the momentum section, where momentum equations are linearized alongside continuity to relate velocity and pressure perturbations, leading to a wave equation for acoustic pressure. Two variations in the models for rectangular and cylindrical coordinates were also explored to offer sine modes and Bessel modes, respectively, to be used in different sections of the engine depending on geometry. Overall, the approach shows that eigenvalues control stability and decay, while eigenfunctions define spatial patterns, providing a unique method for analyzing thermoacoustic instability and heat transfer in rocket engine components. The primary recommendation for the use of this method of finding acoustic pressure oscillations and unsteady heat release is to be used in combination with high computational models and simulations to verify specific sections of the engine that require more in-depth analysis for precise engineering.

Methodology

The energy equation was included to model the thermal effects of combustion and the resulting temperature distribution. It was chosen because temperature changes influence density and the speed of sound, which affect the acoustic response of the system.

General Energy Equation (2d): $$\frac{\partial T}{\partial t} = \alpha\left(\frac{\partial^2 T}{\partial x^2} + \frac{\partial^2 T}{\partial y^2}\right) + \frac{E_v}{\rho C_p}$$

The continuity equation was chosen because it enforces conservation of mass within the combustion chamber. It relates changes in density to the divergence of the velocity field, making it the primary link between fluid motion and pressure fluctuations. This equation is later combined with the momentum equation to produce the acoustic wave equation.

General Continuity Equation (2d): $$\frac{\partial \rho}{\partial t} + \frac{\partial(\rho u)}{\partial x} + \frac{\partial(\rho v)}{\partial y} = 0$$

The momentum equation was selected to describe how pressure gradients create velocity perturbations within the chamber. After linearization, pressure becomes the dominant driving force for the fluid motion. When coupled with the continuity equation, it produces the pressure-based acoustic model used to identify instability.

General Momentum Equation (2d): $$\rho\left(\frac{\partial u}{\partial t} + u \times \nabla u\right) = -\nabla p + \mu\left(\frac{\partial^2 u}{\partial x^2} + \frac{\partial^2 u}{dy^2}\right)$$

Results

Energy Equation Solution

The thermal model produced a temperature field consisting of a dominant steady-state distribution with superimposed transient modes. The steady-state component predicts the highest temperatures near the region of heat generation and decreasing temperature toward the chamber boundaries. The transient modes decayed exponentially, indicating that any initial temperature disturbance becomes less significant over time. Lower-order modes persist the longest and therefore control the overall thermal behavior, while higher-order modes decayed rapidly. In cylindrical sections of the nozzle, the temperature contours become concentrated near the centerline and decrease radially outward according to Bessel-mode behavior.

$$A_{mn} = \frac{4}{L_x \times L_y} \int_0^W \int_0^L f(x,y) \sin\left(\frac{m\pi}{L_x}\right) \sin\left(\frac{n\pi}{L_y}\right) dxdy$$

$$T(x,r,t) = -4\frac{E_v}{k}(x^2 + y^2) + \sum_{m=1}^{\infty}\sum_{n=1}^{\infty} A_{mn}\phi_{mn}(x,y)e^{-\propto\lambda_{mn}t}$$

$$\lambda_{mn} = \left(\frac{\beta_m}{a}\right)^2 + \left(\frac{n\pi}{L}\right)^2 \qquad \phi_{mn}(x,r) = J_0\left(\frac{r}{a}\right)\sin\left(\frac{m\pi x}{L_x}\right)\sin\left(\frac{n\pi y}{L_y}\right)$$

Continuity Equation Solution

The continuity equation derivation shows that pressure and density perturbations remained strongly coupled to the divergence of the velocity field. Regions of positive velocity divergence corresponded to local decreases in density, while regions of negative divergence produced compression. The resulting standing-wave structure form distinct nodal and anti-nodal regions throughout the chamber. The lowest acoustic mode will produce the largest pressure response and therefore dominate the system behavior, whereas higher-order modes generate additional oscillations with smaller spatial wavelengths.

$$\frac{\partial p'}{\partial t} + \nabla(p_o \times u') = 0$$

Momentum Equation Solution

The momentum equation predicts that the largest velocity perturbations occur where pressure gradients are greatest. Combining the momentum and continuity equations produced a set of eigenvalues that identified the stability of each acoustic mode. Modes with negative real eigenvalues decayed and therefore represented stable operating conditions, while modes with positive real eigenvalues grew with time and indicated the onset of thermoacoustic instability. The most unstable modes occurred when the pressure oscillations aligned with regions of heat release, creating strong amplification of the chamber response. The corresponding eigenfunctions showed that velocity oscillations were largest near pressure nodes and smallest near pressure antinodes.

$$p'(x,r,t) = \sum_{m=1}^{\infty}\sum_{n=1}^{\infty} A_{mn} J_0\left(\frac{\beta_m r}{a}\right)\sin\left(\frac{n\pi x}{L_x}\right)[A\cos(\omega t) + B\sin(\omega t)] \qquad \omega = c\sqrt{\left(\frac{\beta_m}{a}\right)^2 + \left(\frac{n\pi}{L_x}\right)^2}$$

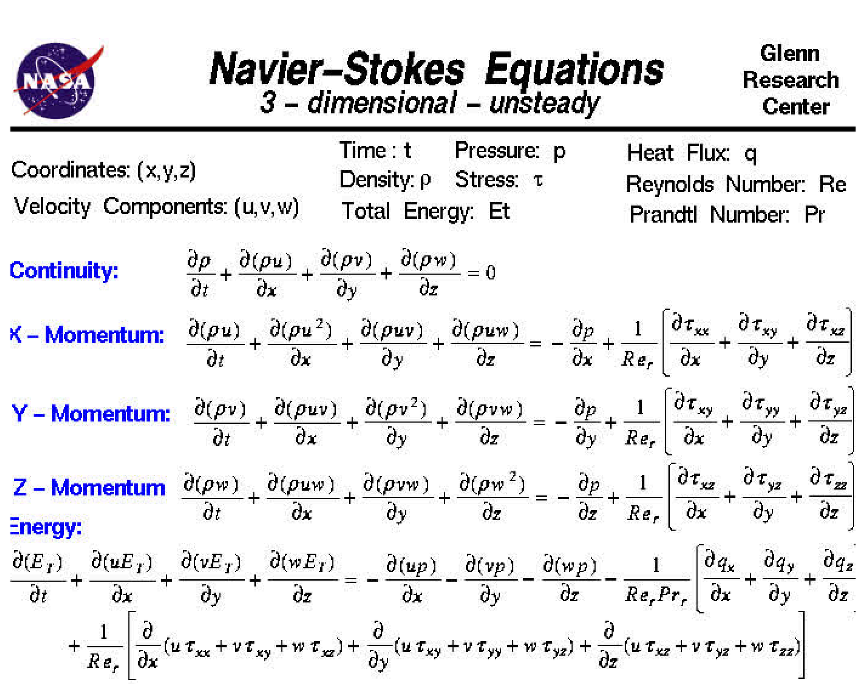

Figure 1. Three-dimensional unsteady form of the Navier–Stokes equations. Adapted from NASA Glenn Research Center (2021).

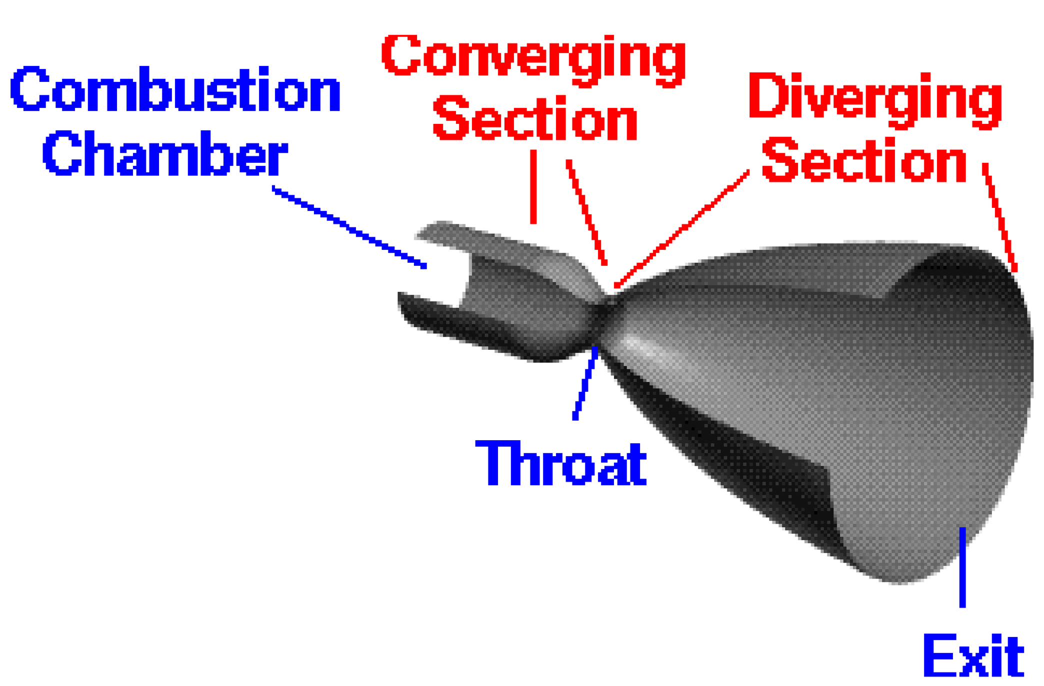

Figure 2. Basic Rocket engine model with nozzle. Photo by NASA GRC Inc.

Conclusion

Future work should focus on extending the present framework to fully couple acoustic pressure and heat release through an analytically derived Rayleigh criterion expressed in terms of the system's eigenmodes. While the current formulation captures pressure and thermal behavior effectively, integrating these components into a unified stability criterion would enhance predictive capability. In addition, implementing numerical methods—such as MATLAB- or Python-based eigenvalue solvers—would enable efficient evaluation of system stability across a range of parameter values and support continued model development as analytical solutions become increasingly unmanageable under coupled conditions.

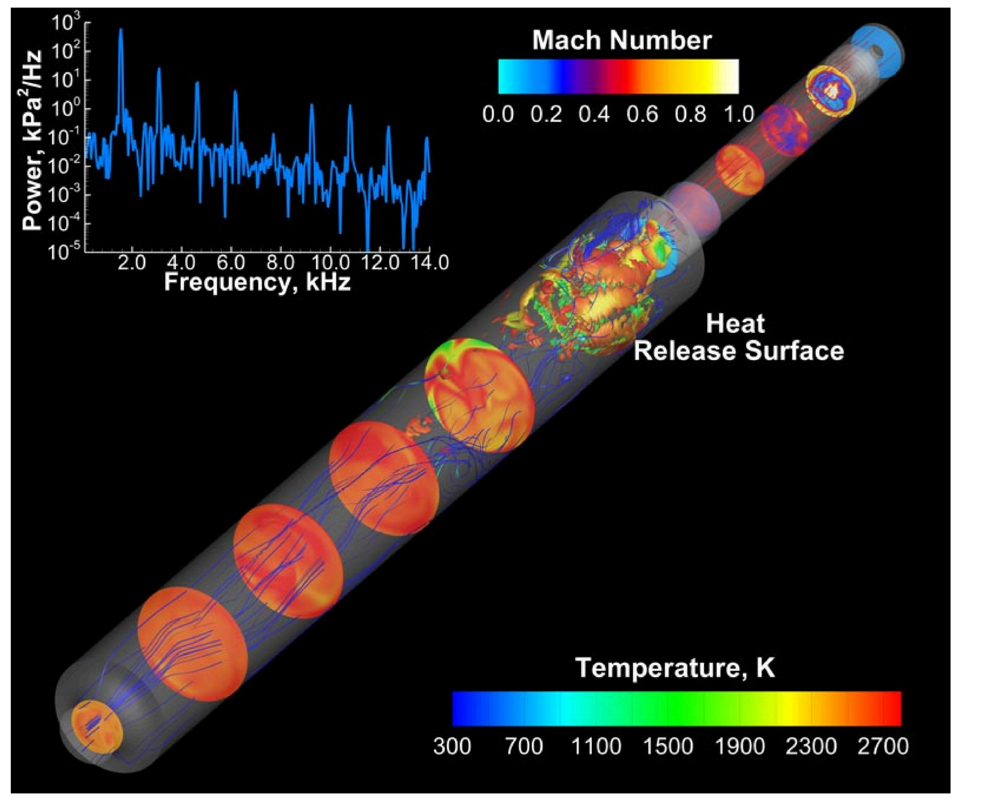

Figure 3. Instantaneous flowfield inside the combustor showing Mach number contours, temperature slices, and combustion heat release. Adapted from NASA Advanced Supercomputing Division (2011).

Further refinement may be achieved by incorporating flame transfer functions to account for time-delayed heat release, thereby enabling formulation of a fully coupled thermoacoustic eigenvalue problem. The inclusion of damping mechanisms would also enhance physical realism by capturing dissipative effects not captured by the current linearized model. Although rectangular and cylindrical domains provide a strong analytical foundation, extending the model to reflect the true geometry of a rocket engine would increase its applicability. Finally, validation through comparison with experimental data and computational fluid dynamics simulations would serve to verify the model and strengthen its relevance to practical engineering systems.

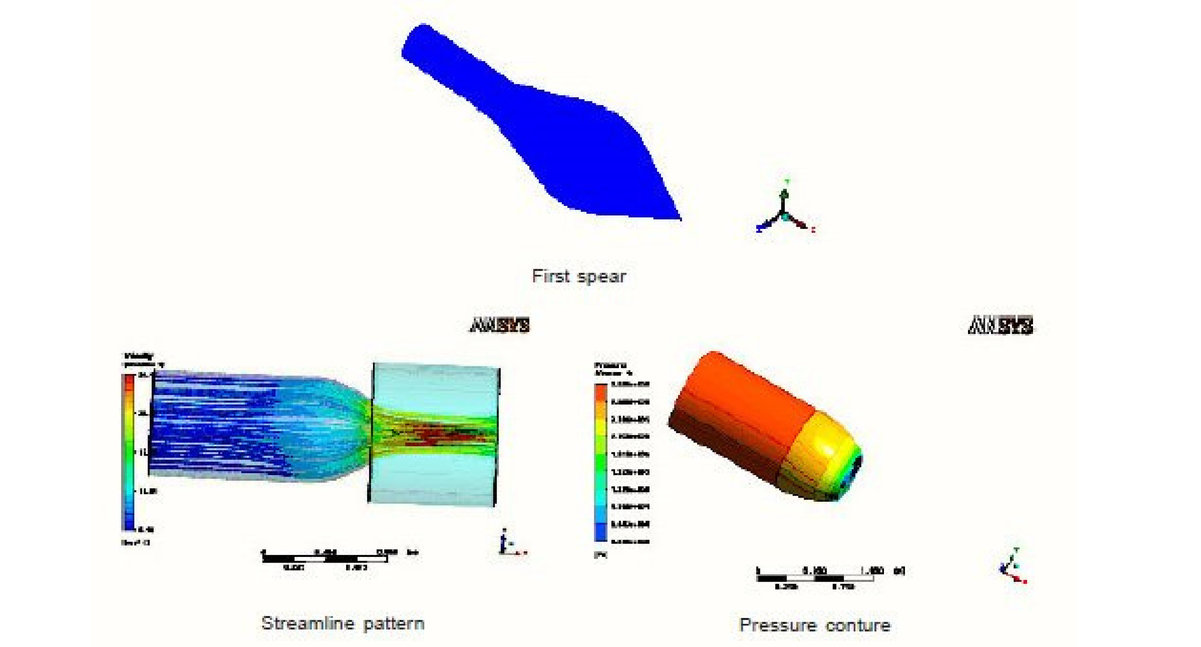

Figure 4. Streamline pattern and pressure contour from a CFD simulation of flow through a converging–diverging rocket nozzle, generated using Ansys. Adapted from Sharma, Prashad, and Kumar (2011).

Sources